Cavin-1/PTRF mediates insulin-dependent focal adhesion remodeling and ameliorates high-fat diet–induced inflammatory responses in mice

Received for publication, April 18, 2019, and in revised form, May 20, 2019 Published, Papers in Press, May 24, 2019, DOI 10.1074/jbc.RA119.008824

Hong Wang[‡1], **Paul F. Pilch**[‡§], **and Libin Liu**[‡¶2]

From the Departments of [‡]*Biochemistry,* [§]*Medicine, and* [¶]*Pharmacology and Experimental Therapeutics, Boston University School of Medicine, Boston, Massachusetts 02118*

Edited by Jeffrey E. Pessin

Cavin-1/polymerase I and transcript release factor (PTRF) is a requisite component of caveolae, small plasma membrane invaginations that are highly abundant in adipocytes. Cavin-1 is a dynamic molecule whose dissociation from caveolae plays an important role in mechanoprotection and rRNA synthesis. In the former situation, the acute dissociation of cavin-1 from caveolae allows cell membrane expansion that occurs upon insulin-aided lipid uptake into the fat cells. Cavin-1 dissociation from caveolae and membrane flattening alters the cytoskeleton and the interaction of plasma membrane proteins with the extracellular matrix through interactions with focal adhesion structures. Here, using cavin-1 knockout mice, subcellular fractionation, and immunoblotting methods, we addressed the relationship of cavin-1 with focal adhesion complexes following nutritional stimulation. We found that cavin-1 is acutely translocated to focal complex compartments upon insulin stimulation, where it regulates focal complex formation through an interaction with paxillin. We found that loss of cavin-1 impairs focal complex remodeling and focal adhesion formation and causes a mechanical stress response, concomitant with activation of proinflammatory and senescence/apoptosis pathways. We conclude that cavin-1 plays key roles in dynamic remodeling of focal complexes upon metabolic stimulation. This mechanism also underlies the crucial role of caveolae in the long-term healthy expansion of the adipocyte.

Caveolae are small flask-shaped invaginations on the plasma membrane that are highly expressed in adipocytes (1–4). Humans with the loss-of-function mutations in the caveolae structural protein–encoding genes *CAV1* encoding caveolin-1 and *PTRF* (polymerase I and transcript release factor) encoding PTRF/cavin-1 and mouse models of caveolae deficiency display lipodystrophic phenotypes, including adipocyte abnormalities, impaired lipid storage, insulin resistance, and other pathologies (5, 6). However, the underlying pathophysiological mechanism(s) for these phenotypes remain incompletely understood. Previous studies have shown that caveolae can serve as a plasma membrane reservoir (7–14), whereby cavin-1 dissociates from caveolae in response to an acute mechanical stress, thus allowing for a significant increase in cell surface area (9, 16). In adipocytes, caveolae play significant roles in normal growth (17–19) and lipid-driven cell size adaptation (20). In a controlled overfeeding clinical trial, caveolin-1 expression at baseline significantly correlated with the degree of adipocyte enlargement among individuals who responded to overfeeding by adipocyte hypertrophy (20). However, the details of cellular and molecular mechanistic regulations are not known.

Cell growth and membrane expansion *in situ* have to be supported by the remodeling of extracellular matrix components, transmembrane adhesion receptors of the integrin family, and integrin-based focal adhesion complexes (21, 22). Upon a diverse range of extracellular stimulations, a number of focal adhesion complex proteins, including focal adhesion kinase (FAK),[3] paxillin, and vinculin, undergo rapid tyrosine phosphorylation, which is accompanied by profound alterations in the organization of the cytoskeleton network and the enhanced assembly of focal adhesion complexes (23, 24). Studies also show that tyrosine phosphorylation of caveolin-1 promotes integrin and focal adhesion dynamics, which plays key roles in mechanosensing and other important biological process (25–27). Here, our studies show in adipocytes that insulin stimulates cavin-1 tyrosine phosphorylation and its translocation from lipid rafts to a focal adhesion complex fraction, where it participates in focal complex formation. By using CRISPR/Cas9 genome-edited cavin-1 null 3T3-L1 adipocytes, we demonstrate that loss of cavin-1 eliminated paxillin phosphorylation but caused FAK hyperactivation in response to hypo-osmotic stress. After a 5-day high-fat diet feeding regimen, compared with WT littermates, cavin-1 null mice showed no increase in adipose tissue weight but showed hyper-FAK phosphorylation, ERK phosphorylation, and pro-inflammatory and apoptotic pathway activation. Collectively, these data support cavin-1 serving as a responder to insulin stimulation and "priming" a pregrowth state by caveolae-focal adhesion and

This work was supported by National Institutes of Health Grant DK-112945 (to P. F. P.). The authors declare that they have no conflicts of interest with the contents of this article. The content is solely the responsibility of the authors and does not necessarily represent the official views of the National Institutes of Health.

This article contains Table S1.

[1] Present address: Broad Institute, Cambridge, MA 02142.

[2] To whom correspondence should be addressed: Dept. of Pharmacology and Experimental Therapeutics, Boston University School of Medicine, Boston, MA 02118. Tel.: 617-358-4203; E-mail: libin@bu.edu.

[3] The abbreviations used are: FAK, focal adhesion kinase; ERK, extracellular signal–regulated kinase; FC, focal complex; PM, plasma membrane; PVDF, phenylmethylsulfonyl fluoride.

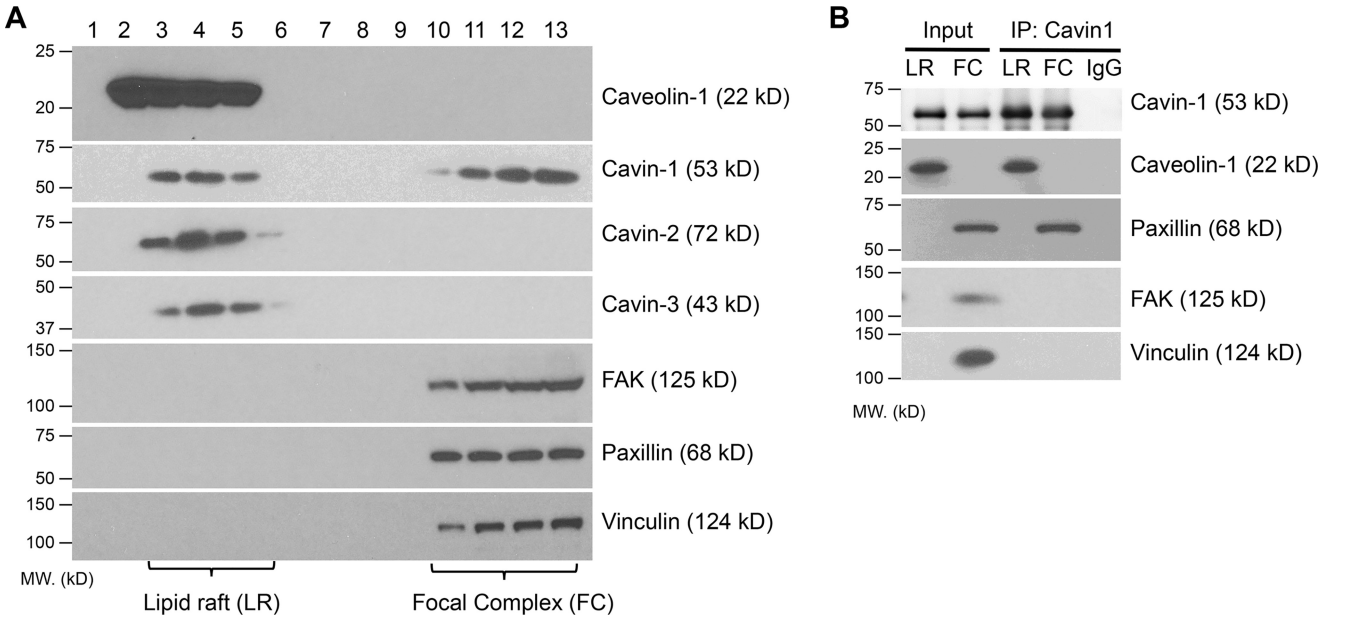

Figure 1. Cavin-1 partially localizes with focal adhesion complex by interacting with paxillin, but not FAK or vinculin. *A*, PM fractions (0.5 mg) obtained from mouse epididymal fat tissue fragments were subjected to lipid raft flotation. Equal volumes of the recovered fractions were separated by SDS-PAGE and transferred to PVDF membrane for immunoblotting analysis using the antibodies indicated. *B*, in the focal complex, cavin-1 binds to paxillin, but not FAK or vinculin. Whole-cell lysates (100 μg of protein) of lipid raft (*LR*) and FC fractions were solubilized in lysis buffer (1% Triton X-100, 150 mM NaCl, 50 mM EDTA) and immunoprecipitated with anti-cavin-1 or nonspecific IgG. After SDS-PAGE, the immunoprecipitations were analyzed by Western blotting with the indicated antibodies, and final detection was done with chemiluminescence.

cytoskeleton remodeling. Loss of this cavin-1–dependent remodeling caused a cell size–induced stress response activation through a FAK signaling pathway and, subsequently, the activation of deleterious pro-inflammatory and cell senescence/apoptotic pathways.

Results

Cavin-1 partially localizes with focal adhesion complex by interacting with paxillin, but not FAK or vinculin

Our previous studies with cultured 3T3-L1 adipocytes and sucrose flotation protocols determined that there was incomplete cavin-1 co-localization with caveolin-1 in the caveolae-enriched lipid raft fractions (28). In other words, a significant amount of cavin-1 remained in the detergent-resistant and nonlipid raft fractions at the bottom of the gradient where cytoskeletal components localize (27). To further evaluate this, we used a primary mouse adipocyte plasma membrane fraction as starting material and performed the lipid raft flotation procedure. Approximately 40–50% of cavin-1 localized in the detergent-resistant, nonlipid raft fraction (Fig. 1*A*). As expected, these fractions were abundant in focal adhesion proteins, including FAK, vinculin, and paxillin (Fig. 1*A*). Therefore, we designated these fractions as a "focal complex" compartment. These data led us to verify the potential interaction between cavin-1 and focal complex components. By co-immunoprecipitation, we identified cavin-1–associated proteins from both detergent-resistant, nonlipid raft and lipid raft fractions. Cavin-1 specifically associated with paxillin, but not with FAK or vinculin (Fig. 1*B*). Overall, these data demonstrate that under basal conditions, a significant amount of cavin-1 localizes in the focal complex compartment through the interaction with paxillin.

Insulin stimulates cavin-1 translocation from caveolae to the focal complex compartment concomitant with its tyrosine phosphorylation

Prior studies have shown that cavin-1 translocates to other cellular compartments upon insulin stimulation (29, 30). To further understand the physiological relevance of the association of cavin-1 with the focal complex, we examined whether cavin-1 localization in the focal complex was regulated by insulin. Indeed, insulin stimulation resulted in cavin-1 redistribution to the focal complex compartment (Fig. 2*A*). Interestingly, we observed that paxillin, which predominantly localizes in the cytosolic fraction, was also significantly recruited to this compartment by insulin. FAK and vinculin showed this trend as well (Fig. 2*A*). The results from a co-immunoprecipitation experiment further confirmed that insulin increased the interaction between cavin-1 and paxillin (Fig. 2*B*). Previously, we have shown that insulin stimulates cavin-1 tyrosine phosphorylation (3, 30). To explore the potential role of cavin-1 tyrosine phosphorylation in its focal complex localization, we examined the cavin-1 tyrosine phosphorylation levels in lipid raft and focal complex fractions. Cavin-1 was predominantly tyrosine-phosphorylated in the focal complex fraction (Fig. 2*C*). The relative ratio of the phosphorylated form to total protein level in the focal complex was 6-fold higher than in the lipid raft fraction (Fig. 2*C*).

Cavin-1 plays a critical role in focal complex stabilization and mediates insulin-stimulated focal complex (FC) remodeling and focal adhesion signal transduction

To investigate the role of cavin-1 in focal adhesion complex formation, we examined basal focal adhesion complex formation in previously characterized CRISPR/Cas9 genome-edited

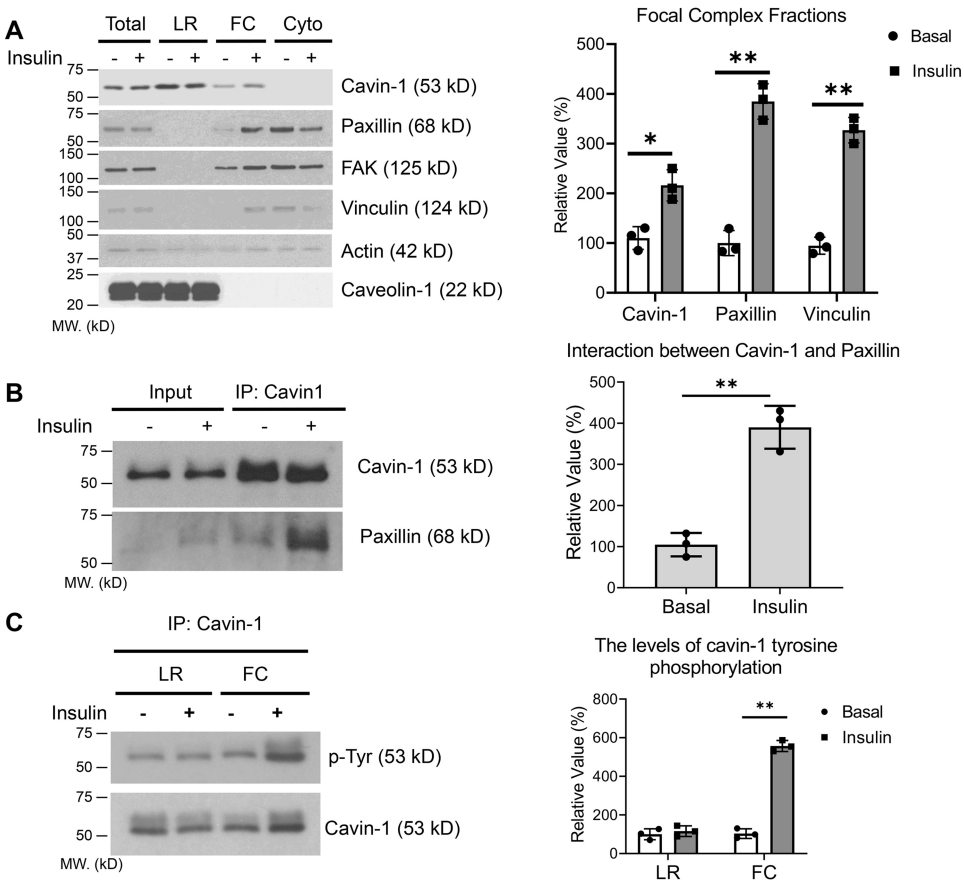

Figure 2. Insulin stimulates cavin-1 translocation and FC formation. Mouse epididymal fat fragments were treated with control or 100 nM insulin followed by fractionation and flotation protocols (see details under "Experimental procedures"). *A*, equal proportions of total plasma membrane (*Total*), lipid rafts (*LR*), FC, and cytosol (*Cyto*; 100× diluted due to the large buffer volume needed for fractionation) were separated by SDS-PAGE and transferred to PVDF for immunoblotting analysis using the antibodies indicated. *B*, whole-plasma membrane fractions were solubilized in lysis buffer (1% Triton X-100, 150 mM NaCl, 50 mM EDTA) and immunoprecipitated (*IP*) with anti-cavin-1 or nonspecific IgG. After SDS-PAGE, the immunoprecipitations were analyzed by Western blotting with the indicated antibodies, and final detection was done with chemiluminescence. *C*, insulin-stimulated cavin-1 tyrosine phosphorylation accumulates with focal complex. Lipid raft and FC fractions from fat tissue fragments stimulated by insulin or not were solubilized in lysis buffer (1% Triton X-100, 150 mM NaCl, 50 mM EDTA) and immunoprecipitated with anti-cavin-1 or nonspecific IgG. After SDS-PAGE, the immunoprecipitations were analyzed by Western blotting with the indicated antibodies, and final detection was done with chemiluminescence. *, $p < 0.05$; **, $p < 0.01$, Student's *t* test. *Error bars*, S.D.

cavin-1 null 3T3-L1 adipocytes and control WT cells (30). Cavin-1 null adipocytes exhibited the same or a slightly higher level of total FAK, paxillin, and vinculin protein expression (Fig. 3*A*); however, their cellular distributions were significantly down-regulated in FC fractions. Further investigations showed that most proteins were mislocated into soluble cytosolic fractions (Fig. 3*A*). These results support cavin-1 playing a key role in focal complex stability and complex formation.

Previous studies in adipocytes have shown that insulin stimulation causes dramatic cytoskeleton network remodeling (31–33). By using paxillin Tyr-118 phospho-antibody, we observed a significant band mobility shift of paxillin on SDS-PAGE (Fig. 3*B*), suggesting that phosphorylation or another acute post-translation modification might also be involved. Lack of cavin-1 caused this band shift to be eliminated (Fig. 3*B*), which suggests that cavin-1–paxillin interaction might serve regulatory roles for downstream focal adhesion signal transduction.

Cavin-1–mediated focal adhesion regulation plays a key role in acute mechanical stress response caused by osmotic swelling

To further investigate the cellular functions of cavin-1 and focal adhesion complex regulation in mechanosensing, we treated WT 3T3-L1 adipocytes with hypo-osmotic medium (a 5× dilution in H_2O of regular culture medium). FAK, paxillin, and cavin-1 disassociated from both lipid raft and focal complex fractions (Fig. 4*A*). Furthermore, two of the known downstream targets of focal adhesion signaling pathway, p38 mitogen-activated protein kinase and ERK, were activated in cavin-1 null adipocytes, showing higher phosphorylation levels under basal conditions and hyperactivation by hypo-osmotic stress (Fig. 4*B*). However, paxillin tyrosine phosphorylation was not regulated by acute hypo-osmotic stress (Fig. 4*B*). These results, together with the results from cavin-1 null adipocytes, support the notion that cavin-1 plays a critical role mediating the osmotic stress, membrane-remodeling response in adipocytes.

Cavin-1 plays a critical role in mature adipocyte expansion through the regulation of focal adhesion remodeling

Cavin-1 null knockout mice show a lipodystrophic phenotype and have a dramatically decreased mature adipocyte size (18). This phenotype has been attributed to disruption of multiple cellular functions, including lipid trafficking (34) and rRNA transcription (30), but the possible role of mechanosensing in the molecular mechanism of mature adipocyte expansion

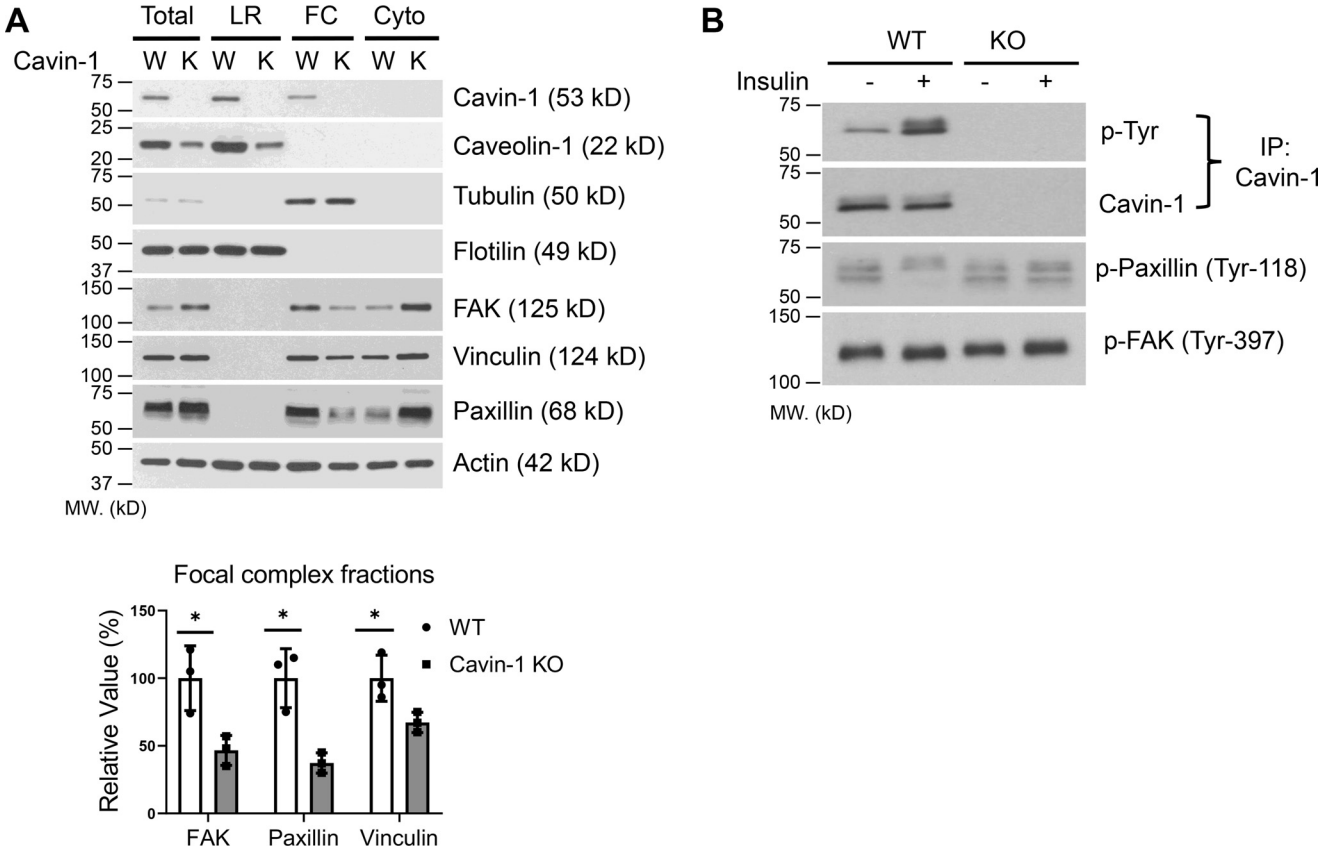

Figure 3. Impaired focal complex formation in cavin-1 null 3T3-L1 adipocytes. *A*, WT (*W*) and cavin-1 null (*K*) 3T3-L1 adipocytes were subjected to the fractionation and flotation protocol (see details under "Experimental procedures"). Equal proportions of total plasma membrane (*Total*), lipid rafts (*LR*), FC, and cytosolic (*Cyto*; 20× diluted due to the large buffer volume needed for fractionation) were separated by SDS-PAGE and transferred to PVDF for immunoblotting analysis using the antibodies indicated. *B*, insulin-stimulated paxillin tyrosine phosphorylation depends on cavin-1 in 3T3-L1 adipocytes. Plasma membrane fractions from cultured 3T3-L1 adipocytes stimulated by insulin or not were solubilized in lysis buffer (1% Triton X-100, 150 mM NaCl, 50 mM EDTA) and immunoprecipitated (*IP*) with anti-cavin-1 or nonspecific IgG. After SDS-PAGE, the immunoprecipitations were analyzed by Western blotting with the indicated antibodies (*top two panels*). Tyrosine-phosphorylated paxillin and FAK were examined by using specific antibodies in equal proportion of total plasma membrane samples (*bottom two panels*). *, $p < 0.05$; Student's *t* test. *Error bars*, S.D.

has not been fully addressed. We challenged WT and cavin-1 null mice with high-fat (60% fat) feeding for 5 days and observed a 2-fold increase in epididymal fat weight in WT mice, whereas cavin-1 null mice did not show any tissue weight gain (Fig. 5*A*). For focal adhesion signaling transduction, FAK tyrosine phosphorylation was activated by high-fat diet feeding in both WT and cavin-1 null mice, but cavin-1 null mice showed a much higher level of activation (Fig. 5*B*). A paxillin phosphorylation band shift was only observed in WT and not in cavin-1 null mice, which is consistent with the results from cultured adipocytes under hypo-osmotic stress (Fig. 4). Furthermore, p38 and ERK exhibited increased activation in cavin-1 null adipocytes, compared with WT. In addition, pro-inflammatory and cell senescence/apoptosis genes were up-regulated in cavin-1 null adipose tissue and superactivated after high-fat diet feeding (Fig. 5*C*). Together with the results from cell culture studies, these data support a model whereby cavin-1 acts as a key regulator of cellular stress through focal complex formation and signaling transduction upon adipocyte expansion–dependent mechanical stress. Loss of cavin-1 impairs focal complex formation and causes the activation of a stress response, which may lead to growth arrest and cell senescence as well as an inflammatory response.

Discussion

In obesity, adipocyte lipid accumulation results in large-scale increased intracellular volume. This process requires the cooperation of multiple cellular adaptations, including lipogenesis, protein biogenesis, and others so that insulin sensitivity can be maintained in a healthy way. One critical factor is the concomitant adaptations of cellular architecture, especially cell membrane expansion. Highly active remodeling in the plasma membrane bilayer upon lipid accumulation is a precondition for maintaining a healthy metabolic responsive state; however, the underlying molecular regulations have not been fully understood. This study demonstrated that cavin-1 serves as a signal transduction molecule that mediates insulin signaling and cell membrane architecture remodeling, including the dynamic change of caveolae and the formation of the focal adhesion complex. Adipocyte hyperplasia starts from the supply of nutrients and insulin stimulation of their uptake. Our studies indicate the existence of an acute cell membrane–remodeling response in adipocytes, which could be crucial for mediating the dynamics of caveolae cycling and focal adhesion formation to further support the expansion of the cell membrane. This is a "priming" state for increasing cellular lipid accumulation,

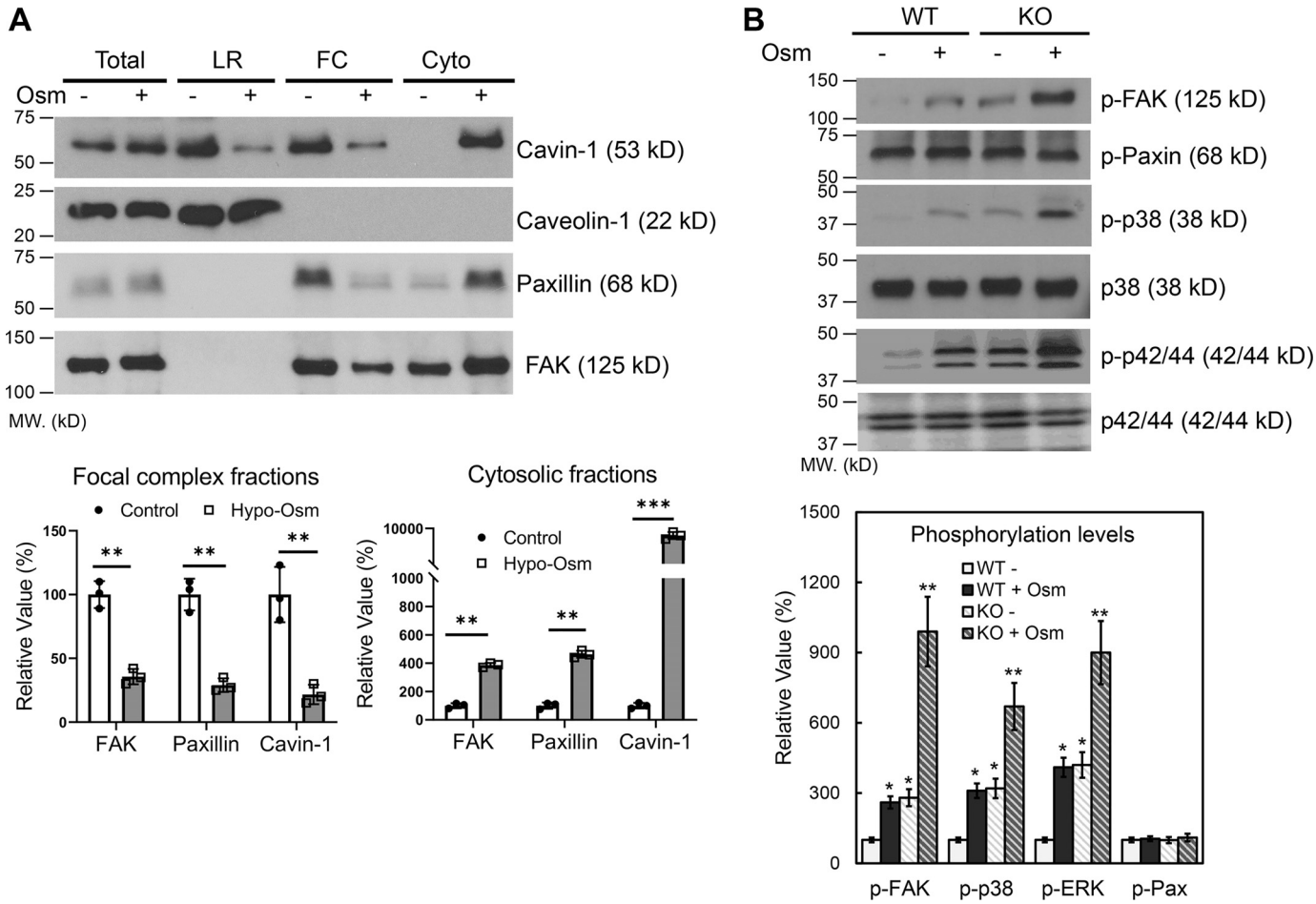

Figure 4. Cavin-1–mediated focal adhesion regulation plays a key role in acute mechanical stress response caused by osmotic swelling. *A*, 3T3-L1 adipocytes were incubated with 1× or 0.2× diluted cell culture medium for 30 min and then subjected to the fractionation and flotation protocol (see details under "Experimental procedures"). Equal proportions of total plasma membrane (*Total*), lipid rafts (*LR*), FC, and cytosol (*Cyto*; 20× diluted due to the large buffer volume needed for fractionation) were separated by SDS-PAGE and transferred to PVDF for immunoblotting analysis using the antibodies indicated. *B*, whole-cell lysates from WT or cavin-1 null (*KO*) 3T3-L1 adipocytes incubated in regular or hypo-osmotic (*Osm*; 5× H_2O-diluted for 30 min) cultured medium were separated by SDS-PAGE and transferred to PVDF for immunoblotting analysis using the antibodies indicated. *, $p < 0.05$; **, $p < 0.01$; ***, $p < 0.001$ Student's *t* test. *Error bars*, S.D.

which is essential for maintaining the healthy insulin-sensitive state in adipocytes. Cavin-1 may serve as a signaling molecule for downstream focal adhesion signal transduction, specifically through the interaction with paxillin. Caveolae deficiency caused the loss of this remodeling response and impaired membrane expansion, therefore imposing mechanical stress directly on focal adhesion complexes and activating a FAK-mediated stress response. In turn, caveolae deficiency will ultimately lead to the activation of downstream pro-apoptosis and pro-inflammatory genes and result in the development of pathological cycles of adipocyte dysfunction. This process is depicted schematically in Fig. 6. This mechanism also provides an additional explanation for the lipodystrophic phenotype observed in caveolae-deficient animal models and human patients with loss-of-function of mutations in *CAV1* and *PTRF* genes. However, this does not exclude the contributions of other mechanisms, such as lipid trafficking (34–36) and ribosome biogenesis (30). Considering the significant role of cavin-1 in the nucleus for rRNA transcription (37–39), it is very possible that cavin-1 plays multiple roles in both the plasma membrane and nucleus. The relationship among lipid raft, focal adhesion complex, and nucleus of cavin-1 translocations remains unclear. It will be interesting to test whether one could serve as the intermediate step for the others and a complete cycle can be established in future studies.

Cavin-1 plays a critical role in caveolae formation (17, 28, 40). Knockout of cavin-1 in a mouse model causes complete lack of caveolae structure in almost all of the tissues (17). Cavin-1 predominantly localizes to the plasma membrane, but it is not a transmembrane protein. It forms a protein complex that is responsible for generating caveolae (28, 41–43). In adipocytes, insulin stimulates cavin-1 translocation outside the lipid raft to other cellular compartments, such as focal adhesion complex and the nucleus (30, 44). These translocations appear to be dependent on its tyrosine phosphorylation (30), and whereas our data show the phosphorylated form of cavin-1 accumulated in focal adhesion complex, the relevant kinase and location where the phosphorylation occurs remain unclear. It has been reported that caveolin-1 is also tyrosine-phosphorylated and localizes to focal adhesions (45–48). However, due to the uncertainty of phospho-caveolin-1 antibody (49), we were unable to confidently verify these results. Further studies are needed to address this question. It is very possible that cavin-1 tyrosine

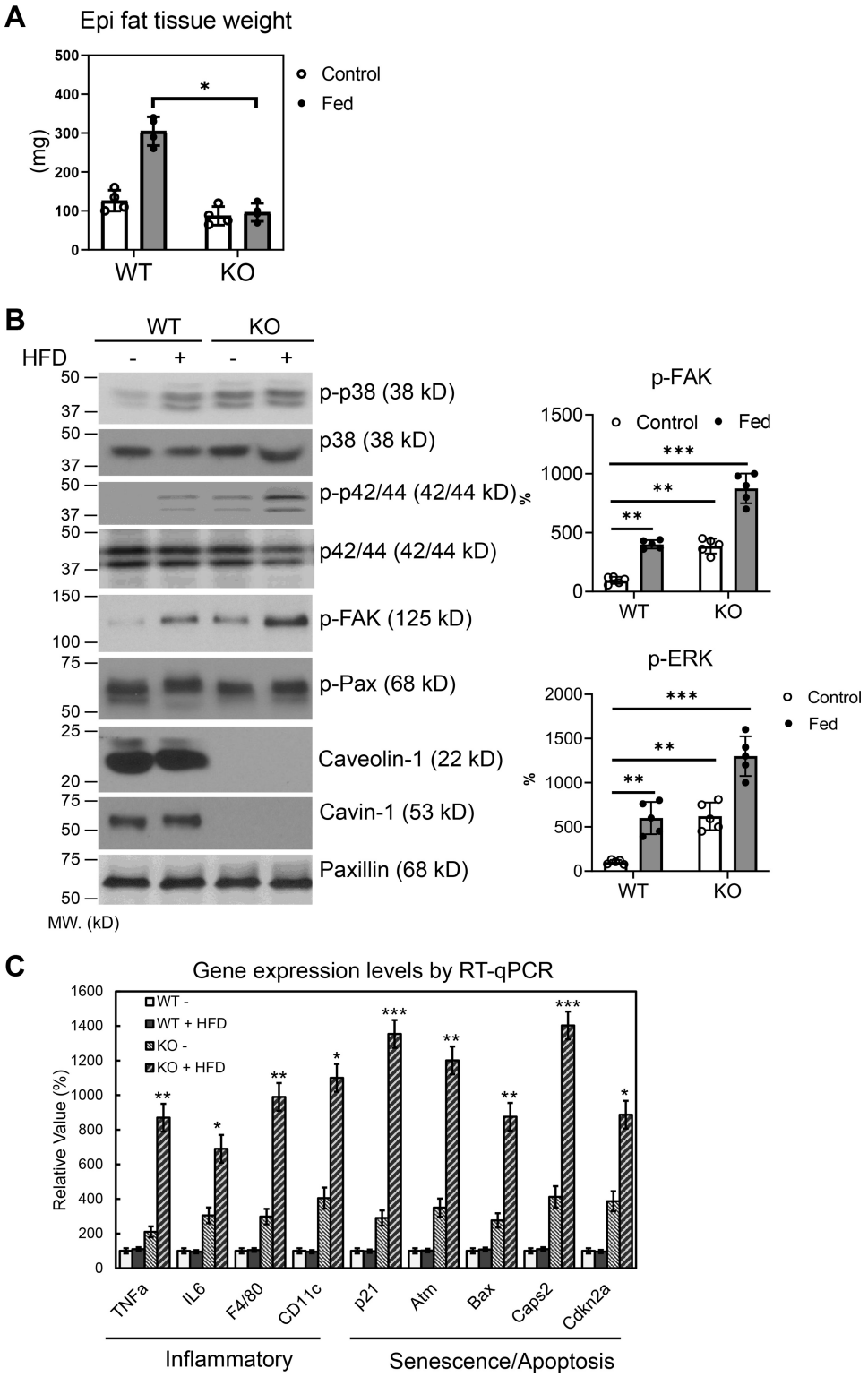

Figure 5. Cavin-1 plays a critical role in mature adipocyte expansion through the regulation of focal adhesion remodeling. *A*, compared with WT mice, cavin-1 null (*KO*) mice have diminished ability of fat tissue expansion upon short-term high-fat diet feeding. Epididymal (*Epi*) fat tissue weight was measured from four groups of mice: before and after 5 days of high-fat (60%) diet feeding, in WT or KO mice, respectively. *B*, whole-epididymal fat tissue lysates from WT or cavin-1 null mice were separated by SDS-PAGE and transferred to PVDF for immunoblotting analysis using the antibodies indicated. *C*, total RNA samples were prepared from epididymal fat tissue lysates from WT or cavin-1 null mice. Gene expression levels were measured by quantitative RT-PCR. *, $p < 0.05$; **, $p < 0.01$; ***, $p < 0.001$, Student's *t* test. *Error bars*, S.D.

phosphorylation occurs within the focal adhesion complex, because multiple signaling factors can be assembled there, whereas caveolae lack direct association with the insulin signaling pathway (50). The recruitment of cavin-1 into focal adhesion complex seems to involve complex formation and downstream signaling transduction, because without cavin-1, the

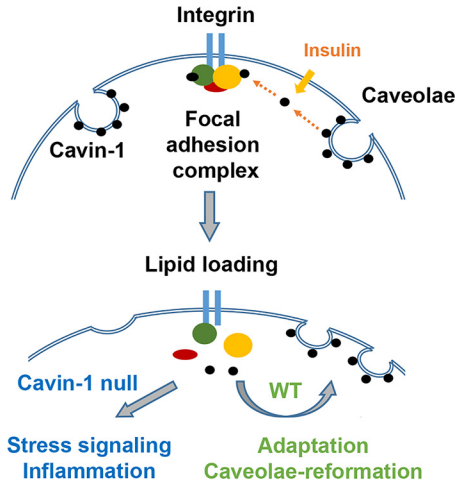

Figure 6. Working model. Under normal conditions, insulin stimulates cavin-1 translocation from caveolae to focal adhesions, which facilitate complex formation and focal adhesion remodeling. Under mechanical stress conditions (physiologically, adipocyte hypertrophy), cavin-1 disassociates from caveolae and is unable to translocate to focal adhesions, which causes instability of complex formation and activation of downstream stress signaling pathways. This may contribute to the development of inflammation and fibrosis that are observed in obese adipocytes.

insulin-dependent phosphorylation of paxillin is diminished. Previous studies have suggested that paxillin plays important roles regulating the FAK-signaling pathway (51, 52). Consistent with this, we observed hyperactivation of FAK phosphorylation and phosphorylation of ERK and p38. In the short term of high-fat diet animal studies, adipose tissue from cavin-1 knockout shows elevated gene expression levels for pro-apoptosis and pro-inflammatory response. These results can explain the inflammation and fibrosis phenotypes observed in a cavin-1–deficient animal model.

Experimental procedures

Cavin-1 knockout mice were created as described previously (17). They were backcrossed for at least eight generations with the C57BL/6 lineage. The mice used in the present study were homozygous male cavin-1 knockout and their WT littermates, which were maintained in a pathogen-free animal facility at 21 °C under a 12-h light/12-h dark cycle with access to a chow diet (catalog no. 2918; Harlan Teklad Global Diet, Madison, WI). In the feeding studies, the mice were fed normal chow (10% fat, D12450B, Research Diets, Inc.) or a high-fat diet (60% fat, D12492, Research Diets, Inc.). Except when specifically noted, all mice used for *in vivo* or *in vitro* studies were fasted for 4–6 h starting from early morning prior to use. For tissue harvesting, mice were euthanized under CO_2, and tissues were rapidly isolated and immediately frozen in liquid nitrogen and stored at −80 °C until further biochemical analysis. All animal studies were performed in accordance with the guidelines and with approval of the Institutional Animal Care and Use Committee of the Boston University School of Medicine.

Reagents

Dexamethasone, 3-isobutylmethylxanthine, insulin, and mouse IgG were purchased from Sigma. Fetal bovine serum (Australian origin) and calf serum were purchased from Thermo Fisher Scientific. Dulbecco's modified Eagle's medium was from Mediatech (Herndon, VA). A BCA protein assay kit was from Pierce. Protein A or G magnetic beads were from Santa Cruz Biotechnology, Inc. Penicillin, streptomycin, and trypsin were purchased from Thermo Fisher Scientific.

Cell culture

3T3-L1 fibroblast culture and differentiation were described previously (28). Generation of PTRF null 3T3-L1 stable cell lines by CRISPR/Cas9 genomic editing was described (30). These cells were cultured and differentiated as described above.

Subcellular fractionation and lipid raft flotation

This procedure was performed on mouse adipocytes essentially as originally described for rat adipocytes (15). Note that to avoid collagenase digestion and the resultant disruption of plasma membrane–extracellular matrix interactions, we carefully dissected out the main vascular structures from fat tissue and cut the remaining tissues into small pieces and then performed the same steps as in previous studies. By eliminating the harsh effect of collagenase digestion, this modification allowed us to examine the characters of plasma membrane in a relative native state. Briefly, mouse epididymal fat tissues were cut into 2–4-mm fragments. After stimulation with control or 100 nM insulin, tissues were washed by cold HES buffer three times and homogenized with a Teflon-glass tissue grinder in HES buffer. The vascular and other nonadipocyte contents were first removed by a brief spin right after homogenization and later from plasma membrane (PM) fractionation steps, because they usually form pellet below 1.12 M (38.5%) sucrose cushion. Subcellular fractions (PM, internal membranes, and cytosol) were obtained by differential centrifugation and resuspended in HES. Buffers used with subcellular fractionation contained a protease inhibitor mixture from Sigma. The flotation protocol was performed as described in previous studies (28). Briefly, 0.5 g of adipose tissue were lysed in 2 ml of MBS (25 mM MES and 150 mM NaCl, pH 6.5) containing 1% Triton X-100 and supplemented with a protease inhibitor mix (Sigma). The samples were then incubated at 4 °C for 20 min with end-over-end rotation. The solubilized lysates were homogenized with 10 strokes of a Dounce homogenizer, and 1 ml of the homogenate was added to an equal volume of 80% (w/v) sucrose in MBS. The solubilized cells (in 40% sucrose) were placed at the bottom of a centrifuge tube and overlaid successively with 2 ml of 30% sucrose and 1 ml of 5% sucrose (in MBS). After centrifugation at 240,000 × *g* in a Beckman SW55 rotor for 18 h, 0.3–0.4-ml fractions were collected from the bottom of the gradient.

Gel electrophoresis and immunoblotting

Proteins were resolved by SDS-PAGE as described. Gels were transferred to polyvinylidene difluoride (PVDF) membranes pretreated with methanol (Bio-Rad) in 25 mM Tris, 192 mM glycine. Membranes were blocked with 1% BSA in PBS containing 0.1% Tween 20 for 1 h at room temperature. Membranes were then probed with the primary antibodies (listed in Table S1) either overnight at 4 °C or for 2 h at room temperature and incubated with horseradish peroxidase–conjugated secondary antibodies (Sigma). Signals were enhanced with chemilumines-

cence reagents (PerkinElmer Life Sciences) for detection of Western signals using a Fujifilm LAS-4000 scanner or autoradiography film (Molecular Technologies, St. Louis, MO). Quantification of signal intensity was performed by using LAS4000 software or ImageJ from scanned films.

Co-immunoprecipitation

The cell/tissue lysates from specific fractions were solubilized with 1% Triton X-100. Insoluble material was removed by pelleting for 10 min in a microcentrifuge. Mouse cavin-1 antibody and nonspecific mouse IgGs were incubated with the supernatant for 1 h at 4 °C, and then 20–40 μl of protein G magnetic beads were added for 2 h to overnight. The supernatant with unbound proteins was collected, and the beads were washed four times and eluted with SDS-PAGE loading buffer containing 2% SDS.

Statistical analyses

All results are presented as mean ± S.D. p values were calculated by unpaired Student's t test or Bonferroni's multiple-comparison test where appropriate. A p value of <0.05 was considered significant. (*, $p < 0.05$; **, $p < 0.01$; ***, $p < 0.001$). For cultured and primary isolated cells, all experiments were performed independently at least three times. Animal studies were from 4–6 animals/group.

Author contributions—H. W., P. F. P., and L. L. conceptualization; H. W. and L. L. data curation; H. W. and L. L. formal analysis; H. W. and L. L. investigation; H. W. and L. L. methodology; H. W. and L. L. writing-original draft; H. W., P. F. P., and L. L. project administration; P. F. P. and L. L. supervision; P. F. P. and L. L. funding acquisition; P. F. P. and L. L. writing-review and editing; L. L. resources.

References

1. Palade, G. E. (1953) Fine structure of blood capillaries. *J. Appl. Physics.* **24,** 1424
2. Yamada, E. (1955) The fine structure of the gall bladder epithelium of the mouse. *J. Biophys. Biochem. Cytol.* **1,** 445–458 CrossRef Medline
3. Pilch, P. F., Souto, R. P., Liu, L., Jedrychowski, M. P., Berg, E. A., Costello, C. E., and Gygi, S. P. (2007) Cellular spelunking: exploring adipocyte caveolae. *J. Lipid Res.* **48,** 2103–2111 CrossRef Medline
4. Parton, R. G. (2018) Caveolae: structure, function, and relationship to disease. *Annu. Rev. Cell Dev. Biol.* **34,** 111–136 CrossRef Medline
5. Patni, N., and Garg, A. (2015) Congenital generalized lipodystrophies–new insights into metabolic dysfunction. *Nat. Rev. Endocrinol.* **11,** 522–534 CrossRef Medline
6. Pilch, P. F., and Liu, L. (2011) Fat caves: caveolae, lipid trafficking and lipid metabolism in adipocytes. *Trends Endocrinol. Metab.* **22,** 318–324 CrossRef Medline
7. Dulhunty, A. F., and Franzini-Armstrong, C. (1975) Relative contributions of folds and caveolae to surface membrane of frog skeletal-muscle fibers at different sarcomere lengths. *J. Physiol.* **250,** 513–539 CrossRef Medline
8. Sinha, B., Köster, D., Ruez, R., Gonnord, P., Bastiani, M., Abankwa, D., Stan, R. V., Butler-Browne, G., Vedie, B., Johannes, L., Morone, N., Parton, R. G., Raposo, G., Sens, P., Lamaze, C., and Nassoy, P. (2011) Cells respond to mechanical stress by rapid disassembly of caveolae. *Cell* **144,** 402–413 CrossRef Medline
9. Lo, H. P., Nixon, S. J., Hall, T. E., Cowling, B. S., Ferguson, C., Morgan, G. P., Schieber, N. L., Fernandez-Rojo, M. A., Bastiani, M., Floetenmeyer, M., Martel, N., Laporte, J., Pilch, P. F., and Parton, R. G. (2015) The caveolin-cavin system plays a conserved and critical role in mechanoprotection of skeletal muscle. *J. Cell Biol.* **210,** 833–849 CrossRef Medline
10. Cheng, J. P. X., Mendoza-Topaz, C., Howard, G., Chadwick, J., Shvets, E., Cowburn, A. S., Dunmore, B. J., Crosby, A., Morrell, N. W., and Nichols, B. J. (2015) Caveolae protect endothelial cells from membrane rupture during increased cardiac output. *J. Cell Biol.* **211,** 53–61 CrossRef Medline
11. Lim, Y. W., Lo, H. P., Ferguson, C., Martel, N., Giacomotto, J., Gomez, G. A., Yap, A. S., Hall, T. E., and Parton, R. G. (2017) Caveolae protect notochord cells against catastrophic mechanical failure during development. *Curr. Biol.* **27,** 1968–1981.e7 CrossRef Medline
12. Yeow, I., Howard, G., Chadwick, J., Mendoza-Topaz, C., Hansen, C. G., Nichols, B. J., and Shvets, E. (2017) EHD proteins cooperate to generate caveolar clusters and to maintain caveolae during repeated mechanical stress. *Curr. Biol.* **27,** 2951–2962.e5 CrossRef Medline
13. Yang, L., and Scarlata, S. (2017) Super-resolution visualization of caveola deformation in response to osmotic stress. *J. Biol. Chem.* **292,** 3779–3788 CrossRef Medline
14. Garcia, J., Bagwell, J., Njaine, B., Norman, J., Levic, D. S., Wopat, S., Miller, S. E., Liu, X., Locasale, J. W., Stainier, D. Y. R., and Bagnat, M. (2017) Sheath cell invasion and trans-differentiation repair mechanical damage caused by loss of caveolae in the zebrafish notochord. *Curr. Biol.* **27,** 1982–1989.e3 CrossRef Medline
15. Jedrychowski, M. P., Gartner, C. A., Gygi, S. P., Zhou, L., Herz, J., Kandror, K. V., and Pilch, P. F. (2010) Proteomic analysis of GLUT4 storage vesicles reveals LRP1 to be an important vesicle component and target of insulin signaling. *J. Biol. Chem.* **285,** 104–114 CrossRef Medline
16. Golani, G., Ariotti, N., Parton, R. G., and Kozlov, M. M. (2019) Membrane curvature and tension control the formation and collapse of caveolar superstructures. *Dev. Cell* **48,** 523–538.e4 CrossRef Medline
17. Liu, L., Brown, D., McKee, M., Lebrasseur, N. K., Yang, D., Albrecht, K. H., Ravid, K., and Pilch, P. F. (2008) Deletion of Cavin/PTRF causes global loss of caveolae, dyslipidemia, and glucose intolerance. *Cell Metab.* **8,** 310–317 CrossRef Medline
18. Ding, S. Y., Lee, M. J., Summer, R., Liu, L., Fried, S. K., and Pilch, P. F. (2014) Pleiotropic effects of cavin-1 deficiency on lipid metabolism. *J. Biol. Chem.* **289,** 8473–8483 CrossRef Medline
19. Martin, S., Fernandez-Rojo, M. A., Stanley, A. C., Bastiani, M., Okano, S., Nixon, S. J., Thomas, G., Stow, J. L., and Parton, R. G. (2012) Caveolin-1 deficiency leads to increased susceptibility to cell death and fibrosis in white adipose tissue: characterization of a lipodystrophic model. *PLoS One* **7,** e46242 CrossRef Medline
20. Briand, N., Prado, C., Mabilleau, G., Lasnier, F., Le Lièpvre, X., Covington, J. D., Ravussin, E., Le Lay, S., and Dugail, I. (2014) Caveolin-1 expression and cavin stability regulate caveolae dynamics in adipocyte lipid store fluctuation. *Diabetes* **63,** 4032–4044 CrossRef Medline
21. Hynes, R. O. (2002) Integrins: bidirectional, allosteric signaling machines. *Cell* **110,** 673–687 CrossRef Medline
22. Kleinschmidt, E. G., and Schlaepfer, D. D. (2017) Focal adhesion kinase signaling in unexpected places. *Curr. Opin. Cell Biol.* **45,** 24–30 CrossRef Medline
23. Parsons, J. T., Martin, K. H., Slack, J. K., Taylor, J. M., and Weed, S. A. (2000) Focal adhesion kinase: a regulator of focal adhesion dynamics and cell movement. *Oncogene* **19,** 5606–5613 CrossRef Medline
24. Mitra, S. K., and Schlaepfer, D. D. (2006) Integrin-regulated FAK-Src signaling in normal and cancer cells. *Curr. Opin. Cell Biol.* **18,** 516–523 CrossRef Medline
25. Goetz, J. G., Joshi, B., Lajoie, P., Strugnell, S. S., Scudamore, T., Kojic, L. D., and Nabi, I. R. (2008) Concerted regulation of focal adhesion dynamics by galectin-3 and tyrosine-phosphorylated caveolin-1. *J. Cell Biol.* **180,** 1261–1275 CrossRef Medline
26. Joshi, B., Bastiani, M., Strugnell, S. S., Boscher, C., Parton, R. G., and Nabi, I. R. (2012) Phosphocaveolin-1 is a mechanotransducer that induces caveola biogenesis via Egr1 transcriptional regulation. *J. Cell Biol.* **199,** 425–435 CrossRef Medline
27. Bailey, K. M., and Liu, J. (2008) Caveolin-1 up-regulation during epithelial to mesenchymal transition is mediated by focal adhesion kinase. *J. Biol. Chem.* **283,** 13714–13724 CrossRef Medline
28. Liu, L., and Pilch, P. F. (2008) A critical role of cavin (polymerase I and transcript release factor) in caveolae formation and organization. *J. Biol. Chem.* **283,** 4314–4322 CrossRef Medline

29. Aboulaich, N., Ortegren, U., Vener, A. V., and Strålfors, P. (2006) Association and insulin regulated translocation of hormone-sensitive lipase with PTRF. *Biochem. Biophys. Res. Commun.* **350,** 657–661 CrossRef Medline
30. Liu, L., and Pilch, P. F. (2016) PTRF/Cavin-1 promotes efficient ribosomal RNA transcription in response to metabolic challenges. *Elife* **5,** e17508 CrossRef Medline
31. Liu, L., Jedrychowski, M. P., Gygi, S. P., and Pilch, P. F. (2006) Role of insulin-dependent cortical fodrin/spectrin remodeling in glucose transporter 4 translocation in rat adipocytes. *Mol. Biol. Cell* **17,** 4249–4256 CrossRef Medline
32. Lopez, J. A., Burchfield, J. G., Blair, D. H., Mele, K., Ng, Y., Vallotton, P., James, D. E., and Hughes, W. E. (2009) Identification of a distal GLUT4 trafficking event controlled by actin polymerization. *Mol. Biol. Cell* **20,** 3918–3929 CrossRef Medline
33. Balamatsias, D., Kong, A. M., Waters, J. E., Sriratana, A., Gurung, R., Bailey, C. G., Rasko, J. E., Tiganis, T., Macaulay, S. L., and Mitchell, C. A. (2011) Identification of P-Rex1 as a novel Rac1-guanine nucleotide exchange factor (GEF) that promotes actin remodeling and GLUT4 protein trafficking in adipocytes. *J. Biol. Chem.* **286,** 43229–43240 CrossRef Medline
34. Meshulam, T., Simard, J. R., Wharton, J., Hamilton, J. A., and Pilch, P. F. (2006) Role of caveolin-1 and cholesterol in transmembrane fatty acid movement. *Biochemistry* **45,** 2882–2893 CrossRef Medline
35. Meshulam, T., Breen, M. R., Liu, L., Parton, R. G., and Pilch, P. F. (2011) Caveolins/caveolae protect adipocytes from fatty acid-mediated lipotoxicity. *J. Lipid Res.* **52,** 1526–1532 CrossRef Medline
36. Pilch, P. F., Meshulam, T., Ding, S., and Liu, L. (2011) Caveolae and lipid trafficking in adipocytes. *Clin. Lipidol.* **6,** 49–58 CrossRef Medline
37. Jansa, P., Mason, S. W., Hoffmann-Rohrer, U., and Grummt, I. (1998) Cloning and functional characterization of PTRF, a novel protein which induces dissociation of paused ternary transcription complexes. *EMBO J.* **17,** 2855–2864 CrossRef Medline
38. Jansa, P., and Grummt, I. (1999) Mechanism of transcription termination: PTRF interacts with the largest subunit of RNA polymerase I and dissociates paused transcription complexes from yeast and mouse. *Mol. Gen. Genet.* **262,** 508–514 Medline
39. Jansa, P., Burek, C., Sander, E. E., and Grummt, I. (2001) The transcript release factor PTRF augments ribosomal gene transcription by facilitating reinitiation of RNA polymerase I. *Nucleic Acids Res.* **29,** 423–429 CrossRef Medline
40. Hill, M. M., Bastiani, M., Luetterforst, R., Kirkham, M., Kirkham, A., Nixon, S. J., Walser, P., Abankwa, D., Oorschot, V. M., Martin, S., Hancock, J. F., and Parton, R. G. (2008) PTRF-Cavin, a conserved cytoplasmic protein required for caveola formation and function. *Cell* **132,** 113–124 CrossRef Medline
41. Bastiani, M., Liu, L., Hill, M. M., Jedrychowski, M. P., Nixon, S. J., Lo, H. P., Abankwa, D., Luetterforst, R., Fernandez-Rojo, M., Breen, M. R., Gygi, S. P., Vinten, J., Walser, P. J., North, K. N., Hancock, J. F., *et al.* (2009) MURC/Cavin-4 and cavin family members form tissue-specific caveolar complexes. *J. Cell Biol.* **185,** 1259–1273 CrossRef Medline
42. Gambin, Y., Ariotti, N., McMahon, K. A., Bastiani, M., Sierecki, E., Kovtun, O., Polinkovsky, M. E., Magenau, A., Jung, W., Okano, S., Zhou, Y., Leneva, N., Mureev, S., Johnston, W., Gaus, K., *et al.* (2013) Single-molecule analysis reveals self assembly and nanoscale segregation of two distinct cavin subcomplexes on caveolae. *eLife* **3,** e01434 CrossRef Medline
43. Ludwig, A., Howard, G., Mendoza-Topaz, C., Deerinck, T., Mackey, M., Sandin, S., Ellisman, M. H., and Nichols, B. J. (2013) Molecular composition and ultrastructure of the caveolar coat complex. *PLoS Biol.* **11,** e1001640 CrossRef Medline
44. Wei, Z., Zou, X., Wang, H., Lei, J., Wu, Y., and Liao, K. (2015) The N-terminal leucine-zipper motif in PTRF/cavin-1 is essential and sufficient for its caveolae-association. *Biochem. Biophys. Res. Commun.* **456,** 750–756 CrossRef Medline
45. Joshi, B., Strugnell, S. S., Goetz, J. G., Kojic, L. D., Cox, M. E., Griffith, O. L., Chan, S. K., Jones, S. J., Leung, S. P., Masoudi, H., Leung, S., Wiseman, S. M., and Nabi, I. R. (2008) Phosphorylated caveolin-1 regulates Rho/ROCK-dependent focal adhesion dynamics and tumor cell migration and invasion. *Cancer Res.* **68,** 8210–8220 CrossRef Medline
46. Radel, C., and Rizzo, V. (2005) Integrin mechanotransduction stimulates caveolin-1 phosphorylation and recruitment of Csk to mediate actin reorganization. *Am. J. Physiol. Heart Circ. Physiol.* **288,** H936–H945 CrossRef Medline
47. del Pozo, M. A., Balasubramanian, N., Alderson, N. B., Kiosses, W. B., Grande-García, A., Anderson, R. G. W., and Schwartz, M. A. (2005) Phospho-caveolin-1 mediates integrin-regulated membrane domain internalization. *Nat. Cell Biol.* **7,** 901–908 CrossRef Medline
48. Cao, H., Courchesne, W. E., and Mastick, C. C. (2002) A phosphotyrosine-dependent protein interaction screen reveals a role for phosphorylation of caveolin-1 on tyrosine 14—recruitment of C-terminal Src kinase. *J. Biol. Chem.* **277,** 8771–8774 CrossRef Medline
49. Hill, M. M., Scherbakov, N., Schiefermeier, N., Baran, J., Hancock, J. F., Huber, L. A., Parton, R. G., and Parat, M. O. (2007) Reassessing the role of phosphocaveolin-1 in cell adhesion and migration. *Traffic* **8,** 1695–1705 CrossRef Medline
50. Souto, R. P., Vallega, G., Wharton, J., Vinten, J., Tranum-Jensen, J., and Pilch, P. F. (2003) Immunopurification and characterization of rat adipocyte caveolae suggest their dissociation from insulin signaling. *J. Biol. Chem.* **278,** 18321–18329 CrossRef Medline
51. Burridge, K., Turner, C. E., and Romer, L. H. (1992) Tyrosine phosphorylation of paxillin and pp125FAK accompanies cell adhesion to extracellular matrix: a role in cytoskeletal assembly. *J. Cell Biol.* **119,** 893–903 CrossRef Medline
52. Schaller, M. D. (2001) Paxillin: a focal adhesion-associated adaptor protein. *Oncogene* **20,** 6459–6472 CrossRef Medline